

Thermal field theory and the QCD Equation of State

Matteo Bresciani^{i,a}

Trinity College Dublin, School of Mathematics and Hamilton Mathematics Institute, Dublin, Ireland

© 20xx Elsevier Ltd. All rights reserved.

Contents

Objectives	1
1 Introduction	1
2 QCD thermodynamics	2
3 Thermal effective theory of QCD	3
3.1 Electrostatic QCD	3
3.2 Magnetostatic QCD	4
3.3 The QCD pressure	4
3.4 Scope of the effective theory	4
4 QCD Equation of State	5
4.1 Perturbative methods	5
4.2 Non-perturbative determination	6
4.3 Finite density	7
5 Thermal phases of QCD	7
5.1 The $\mu = 0$ case	8
5.2 The $\mu \neq 0$ case	8
6 Summary	9
Acknowledgement	9
References	9

Abstract

This Chapter introduces QCD at finite temperature and density. We first present the formulation of the thermal theory in the Euclidean path integral formalism. We then describe how the strong dynamics at high temperature can be inspected through thermal effective field theories. As a concrete example of thermodynamic quantity, we discuss the Equation of State, which characterises the equilibrium properties of the QCD plasma. We finally conclude with an overview of the phase diagram of strongly interacting matter.

Keywords: Thermal field theory, QCD, Equation of State, Phase diagram

Objectives

- The formulation of QCD at finite temperature and density is first presented.
- Then, the theoretical tool of the thermal effective theory is introduced to investigate QCD at high temperature.
- The Equation of State is introduced and its determination, both with perturbative and non-perturbative methods, is reviewed.
- The main properties of QCD matter under different regimes of temperature and density are described.

1 Introduction

In the Standard Model, the strong interactions of quarks and gluons are described by Quantum Chromodynamics (QCD). Among the rich spectrum of phenomena arising from QCD, those occurring under extreme conditions of temperature and density are of primary relevance for improving our understanding of Nature, from particle physics to astrophysics. At very high temperatures, QCD matter takes the form of a plasma of quarks and gluons, which is believed to have characterised the Universe in its earliest stages. The opposite regime of cold and very dense matter is instead expected to occur in the core of neutron stars. In particle physics, heavy-ion collision experiments investigate QCD matter close to the conditions where hadrons melt into the plasma phase.

Accurate predictions about QCD thermodynamics are essential for interpreting experimental data [1, 2], and as inputs for the cosmological models [3, 4]. A key theoretical quantity is the Equation of State, which encodes the temperature dependence of the effective degrees of freedom of the QCD plasma. As such, it is crucial for charting the QCD phase diagram at different temperatures and densities. Moreover, the Equation of State directly influenced the expansion of the early Universe and it might have left a distinctive footprint in cosmological observables like the primordial gravitational waves [3].

The aim of this Chapter is to introduce the formalism of QCD thermodynamics and summarise the current understanding of the behaviour of strongly interacting matter at non-zero temperature and density. In Section 2 we set up the theoretical framework of the thermal field

2 Thermal field theory and the QCD Equation of State

theory. Section 3 presents the thermal effective theory approach, a commonly used tool to treat separately contributions from the different thermal scales that characterise QCD at high temperature. This is also a convenient framework for perturbative calculations at finite temperature. Section 4 is dedicated to the Equation of State: we review its determination both in perturbation theory and non-perturbatively using lattice QCD, and discuss the state of the art in the field. Section 5 provides an overview of the present understanding of the QCD phase diagram based on theoretical and experimental results, and highlights some open questions. Finally, Section 6 contains some concluding remarks on the topics discussed throughout the Chapter.

2 QCD thermodynamics

We are interested in the description of a thermal system of interacting quarks and gluons at a temperature T , quark chemical potential μ and in a three-dimensional box of volume V . At the quantum mechanical level, such system is described by the grand-canonical partition function

$$\mathcal{Z} = \text{Tr} \left\{ e^{-\beta(\widehat{H} - \mu\widehat{N})} \right\}, \quad (1)$$

where $\beta = 1/T$ is the inverse temperature ¹, \widehat{H} is the Hamiltonian operator and \widehat{N} is the quark number operator (three times the baryon number). A positive (negative) chemical potential thus represents a net baryon (anti-baryon) number. The trace is taken over all the states in the Hilbert space on which the Hamiltonian \widehat{H} acts. The partition function in Eq. (1) admits a representation in terms of a path integral over the gauge and quark fields in Euclidean spacetime,

$$\mathcal{Z} = \int DAD\bar{\psi}D\psi e^{-S_{\text{QCD}}[A, \bar{\psi}, \psi]}, \quad (2)$$

where $A_\mu(x)$ is the gauge field, $\psi(x), \bar{\psi}(x)$ are the quark and antiquark fields, the action reads

$$S_{\text{QCD}}[A, \bar{\psi}, \psi] = \int_0^\beta dx_0 \int_V d^3\mathbf{x} \mathcal{L}_{\text{QCD}}[A, \bar{\psi}, \psi] \quad (3)$$

and \mathcal{L}_{QCD} is the QCD Lagrangian. The finite temperature thus amounts to restricting the integration over Euclidean time to the interval $0 \leq x_0 \leq \beta$ in the definition of S_{QCD} . Along this compact direction the gauge fields satisfy periodic boundary conditions,

$$A_\mu(x_0 + \beta, \mathbf{x}) = A_\mu(x_0, \mathbf{x}), \quad (4)$$

while the fermionic fields satisfy anti-periodic boundary conditions,

$$\begin{aligned} \psi(x_0 + \beta, \mathbf{x}) &= -\psi(x_0, \mathbf{x}), \\ \bar{\psi}(x_0 + \beta, \mathbf{x}) &= -\bar{\psi}(x_0, \mathbf{x}). \end{aligned} \quad (5)$$

Along the spatial directions, which are assumed to be much larger than the compact one, all the fields satisfy periodic boundary conditions. The thermodynamic average of an observable O is then given by the expectation value

$$\langle O \rangle = \frac{1}{\mathcal{Z}} \int DAD\bar{\psi}D\psi O[A, \bar{\psi}, \psi] e^{-S_{\text{QCD}}[A, \bar{\psi}, \psi]}. \quad (6)$$

As for QCD in the vacuum, the path integral in Eq. (6) can be rigorously defined through the lattice regularization of the theory, a renormalization procedure and the continuum limit. We refer to standard textbooks for the details (for instance, Refs. [5–7]), and use here a formal continuum notation.

Given the partition function we can now introduce the thermodynamic functions, which describe the properties of a plasma of quarks and gluons at equilibrium. The pressure is the most fundamental one, whose expression in the thermodynamic limit (i.e. infinite-volume limit) reads

$$p = \lim_{V \rightarrow \infty} \frac{T}{V} \ln \mathcal{Z}, \quad (7)$$

and represents a counting of the effective degrees of freedom of the thermal system per unit volume. The energy density e , the entropy density s , and the particle density n of the thermal system are respectively defined as

$$e = \lim_{V \rightarrow \infty} \frac{T^2}{V} \frac{\partial}{\partial T} \ln \mathcal{Z}, \quad s = \frac{\partial p}{\partial T}, \quad n = \frac{\partial p}{\partial \mu}. \quad (8)$$

All together, the thermodynamic functions satisfy the relation

$$Ts + \mu n = e + p, \quad (9)$$

¹In particle physics the unit system is chosen such that $c = \hbar = k_B = 1$, where c is the speed of light, \hbar the reduced Planck constant and k_B the Boltzmann constant. All dimensionful quantities can be expressed in terms of one unit only, set to be the electronvolt (eV). In particular, energy and temperature have the same unit. For reference, a temperature of 1 eV corresponds to about 10^5 K.

and their dependence on the external parameters T and μ goes under the name of the Equation of State.

3 Thermal effective theory of QCD

We discuss now a commonly used theoretical framework to study strong interactions at asymptotically high temperatures: the thermal effective theory approach to QCD [8, 9]. In this regime three relevant energy scales emerge: the hard scale, of $O(\pi T)$, the soft scale, of $O(gT)$ where g is the strong coupling, and the ultrasoft scale, of $O(g^2 T)$. Asymptotic freedom guarantees that the three scales are separated for very high temperatures, and the QCD degrees of freedom can be effectively factorised in a similar manner. Physics at long distances with respect to the compact direction (or, equivalently, at low energies with respect to the temperature) can be described by an effective theory whose degrees of freedom are the soft and ultrasoft modes, while the hard modes contribute through the matching coefficients. This effective theory is called Electrostatic QCD. Following similar arguments, Electrostatic QCD can be further reduced to an effective theory for the ultrasoft modes only, called Magnetostatic QCD. Notice that, given the classification of the degrees of freedom, the thermal effective theories can be defined non-perturbatively and are well suited, in principle, for numerical simulations [10, 11]. The thermal effective theory is also the standard framework where perturbative calculations at high temperature are carried out.

3.1 Electrostatic QCD

We consider thermal QCD at zero chemical potential and vanishing quark masses. At very high temperatures asymptotic freedom allows us to treat the theory in the non-interacting case. In momentum space, the free gluon propagator in the Feynman gauge is

$$(D_G)_{\mu\nu}^{ab}(n, \mathbf{p}) = \frac{\delta^{ab} \delta_{\mu\nu}}{|\mathbf{p}|^2 + (2\pi n T)^2}, \quad (10)$$

where a, b are colour indices and n is a non-negative integer labelling the Fourier modes along the compact direction, called Matsubara frequencies. The free (massless) fermion propagator reads

$$D_F(n, \mathbf{p}) = \frac{-i(2n+1)\pi T \gamma_0 - ip_k \gamma_k}{|\mathbf{p}|^2 + [(2n+1)\pi T]^2}, \quad (11)$$

where γ_0 and γ_k , $k = 1, 2, 3$ denote the Dirac matrices and repeated indices are summed. We now consider physics at large distances compared to the size $1/T$ of the compact direction, which means small three-momentum compared to the temperature: $|\mathbf{p}| \ll T$. The fermionic modes are suppressed by the non-vanishing term $(2n+1)\pi T$ (whose $n=0$ contribution can be interpreted as a thermal mass), as well as the gauge modes with $n > 0$: these are called the hard modes. The remaining $n=0$ modes of the gauge field are static, i.e. time-independent, a fact that is known as dimensional reduction. We denote them as $\bar{A}_\mu(\mathbf{x})$, and they represent the field content of a three-dimensional effective theory of QCD holding at energies much lower than T , called Electrostatic QCD (EQCD). Dimensional reduction leads to different gauge transformation rules for electric and magnetic components,

$$\bar{A}'_0(\mathbf{x}) = \Omega(\mathbf{x}) \bar{A}_0(\mathbf{x}) \Omega(\mathbf{x})^\dagger, \quad (12)$$

$$\bar{A}'_j(\mathbf{x}) = \Omega(\mathbf{x}) \bar{A}_j(\mathbf{x}) \Omega(\mathbf{x})^\dagger - \frac{i}{g_E} \Omega(\mathbf{x}) \partial_j \Omega^\dagger(\mathbf{x}), \quad (13)$$

$$\bar{F}'_{jk}(\mathbf{x}) = \Omega(\mathbf{x}) \bar{F}_{jk}(\mathbf{x}) \Omega(\mathbf{x})^\dagger, \quad (14)$$

where g_E is the coupling of EQCD, $\bar{F}_{jk} = (ig_E)^{-1} [D_j, D_k]$ is the field strength tensor associated to \bar{A}_j , $D_j = \partial_j + ig_E \bar{A}_j$ is the covariant derivative, and $\Omega(\mathbf{x}) \in \text{SU}(3)$ is a time-independent gauge transformation. As we will see below, the mass dimension of the coupling g_E is such that $[g_E^2] = 1$. With the chosen conventions, this implies that $[\bar{A}_0] = [\bar{A}_j] = 1/2$. The EQCD Lagrangian includes all the Lorentz and gauge-invariant operators with mass dimension ≤ 3 ,

$$\mathcal{L}_{\text{EQCD}} = \frac{1}{4} \text{tr} \{ \bar{F}_{jk} \bar{F}_{jk} \} + \text{tr} \{ D_j \bar{A}_0 D_j \bar{A}_0 \} + m_E^2 \text{tr} \{ \bar{A}_0^2 \} + \lambda_A \text{tr} \{ \bar{A}_0^2 \}^2 + \dots, \quad (15)$$

and the dots stand for terms with higher mass dimension and thus suppressed by the proper power of $1/T$. As a consequence of dimensional reduction, from Eqs. (12)–(14) it follows that the component \bar{A}_0 effectively behaves as a scalar field in the adjoint representation of the gauge group and therefore it admits a mass m_E , called Debye screening mass. We finally write the action of the effective theory as

$$S_{\text{EQCD}} = \int_V d^3 \mathbf{x} \mathcal{L}_{\text{EQCD}}. \quad (16)$$

In order to match EQCD to QCD, the parameters g_E^2 , m_E and λ_A need to be expressed in terms of the QCD parameters so that, when the same physical quantity is computed in the two theories, the same result is obtained up to temperature-suppressed corrections due to the (infinitely many) higher dimensional operators that have been omitted in the Lagrangian. Then, given the matching, theoretical predictions for static quantities can be obtained by studying the three-dimensional effective theory in place of full QCD [11]. If the matching is determined in perturbation theory, then the EQCD parameters are expressed in terms of the strong coupling g and T . At leading perturbative order and for

4 Thermal field theory and the QCD Equation of State

N_f quark flavours they read [12, 13]

$$g_E^2 = g^2 T, \quad m_E^2 = \frac{1}{3} \left(3 + \frac{1}{2} N_f \right) g^2 T^2, \quad \lambda_A = \frac{1}{4\pi^2} g^4 T. \quad (17)$$

3.2 Magnetostatic QCD

The Debye mass $m_E \sim gT$ and the dimensionful coupling $g_E^2 \sim g^2 T$ provide the two relevant energy scales of EQCD. The former is called soft scale, and it is associated to the electric component \bar{A}_0 of the gauge field. The latter is called ultrasoft scale, and the associated degrees of freedom are the magnetic components \bar{A}_j of the gauge field. For sufficiently high temperatures, phenomena at energies much lower than m_E can be described by an effective theory where the field \bar{A}_0 is static and contributes only through the matching coefficients. This effective theory is called Magnetostatic QCD (MQCD), with action

$$S_{\text{MQCD}} = \int_V d^3 \mathbf{x} \left[\frac{1}{4} \text{tr} \{ \bar{F}_{jk} \bar{F}_{jk} \} + \dots \right], \quad (18)$$

where \bar{F}_{jk} is the strength tensor for the field \bar{A}_j in the fundamental representation of the gauge group. The dots stand for higher dimensional operators suppressed by the proper power of $1/m_E$. MQCD is a three-dimensional SU(3) pure gauge theory, with coupling g_M^2 . The latter must be expressed in terms of the EQCD parameters so that the two theories match. At leading order in perturbation theory, the matching is simply $g_M^2 = g_E^2 = g^2 T$. MQCD is a confining theory; consequently, even in the weak coupling regime of QCD at asymptotically high temperatures, the ultrasoft contributions remain of non-perturbative nature. The only mass scale of the theory is the coupling itself, and therefore every dimensionful quantity in MQCD will be proportional to the proper power of g_M^2 , with a non-perturbative coefficient.

3.3 The QCD pressure

As a showcase, we outline in the following how the thermal effective theories can be employed to separate the hard, soft and ultrasoft contributions in the QCD pressure, defined in Eq. (7). At high temperatures, the pressure can be written as [9]

$$p(T) = T \left(c_E(T) + \frac{1}{V} \log \mathcal{Z}_{\text{EQCD}} \right) \quad (19)$$

(the thermodynamic limit is understood), where $\mathcal{Z}_{\text{EQCD}}$ is the partition function for EQCD,

$$\mathcal{Z}_{\text{EQCD}} = \int D\bar{A}_0 D\bar{A}_j e^{-S_{\text{EQCD}}}, \quad (20)$$

and the action S_{EQCD} is given by Eq. (16). In addition to the matching of the coefficients g_E, m_E, λ_A , we have to match the coefficient c_E as well, that can be interpreted as the unit operator omitted in the effective Lagrangian. In Eq. (19), c_E represents the contribution to the pressure from the hard scale, while the logarithm of the EQCD partition function contains the contributions from the soft and ultrasoft scales. The two latter scales can be separated by introducing MQCD as the effective theory of EQCD at energy scales much smaller than the soft scale. The pressure of QCD can thus be written as

$$p(T) = T \left(c_E(T) + c_M(T) + \frac{1}{V} \log \mathcal{Z}_{\text{MQCD}} \right), \quad (21)$$

where $\mathcal{Z}_{\text{MQCD}}$ is the partition function for MQCD,

$$\mathcal{Z}_{\text{MQCD}} = \int D\bar{A}_j e^{-S_{\text{MQCD}}}, \quad (22)$$

and the action S_{MQCD} is given by Eq. (18). Again, in addition to the matching of the coupling g_M , the coefficient c_M must be matched as well. In Eq. (21), c_M represents the contribution to the pressure from the soft scale, while the logarithm of the MQCD partition function contains the contribution from the ultrasoft scale. The latter must be determined non-perturbatively in MQCD, which is a three-dimensional Yang-Mills theory and thus it is much simpler to simulate on the lattice with respect to full QCD [10]. Then, given the matching of all the parameters, Eq. (21) yields the pressure of full QCD in the high temperature regime.

The matching of the parameters has been determined in perturbation theory, see Ref. [14] for a review. Actually Eq. (21) is the starting point for the computation of the pressure in thermal perturbation theory, as we will discuss later.

3.4 Scope of the effective theory

The effective theory approach holds under the assumption that the hard, soft and ultrasoft energy scales are well separated among each other, so that the relative degrees of freedom can be effectively factorised. In other words, the hierarchy of scales

$$g^2 T / \pi \ll gT \ll \pi T \quad (23)$$

must be respected. The strong coupling g is a function of a renormalization scale $\bar{\mu}$, and the well-known leading order expression for the three-flavour theory is

$$\frac{1}{g^2(\bar{\mu})} = \frac{9}{8\pi^2} \ln(\bar{\mu}/\Lambda) + \dots, \quad (24)$$

where Λ is the QCD Lambda-parameter. In the $\overline{\text{MS}}$ scheme, and for $N_f = 3$, $\Lambda_{\overline{\text{MS}}} = 341$ MeV [15]. In the context of thermal QCD, it is natural to choose the renormalization scale to be proportional to the temperature. The usual choice for the scale is the lowest non-vanishing Matsubara frequency of the gluon modes, $\bar{\mu} = 2\pi T$. Then, the coupling is a logarithmically decreasing function of T , and for sufficiently high temperatures the hierarchy (23) will be in place. For reference, the value of the running coupling of QCD with three flavours, renormalized in the $\overline{\text{MS}}$ scheme, is of $O(1)$ at the electroweak scale, of $O(100)$ GeV. This might signal that only in the very high temperature regime the inequalities (23) are actually respected.

4 QCD Equation of State

The QCD Equation of State (EoS), introduced in Section 2, is a fundamental theoretical quantity that describes the collective behaviour of a strongly interacting plasma at equilibrium. It is a key input for the analysis of data produced in heavy ion colliders [1, 2], as well as for understanding the thermal expansion of the early Universe [3, 4]. We will first discuss the methods that have been developed for the determination of the EoS at vanishing chemical potential, both perturbatively and non-perturbatively. We will then comment on the extension of these results to the case of a non-vanishing chemical potential.

4.1 Perturbative methods

In QCD, asymptotic freedom in principle allows phenomena occurring at very high energy scales to be described using perturbation theory. In the thermal theory, the temperature is the natural energy scale. However, perturbative calculations at finite temperature are plagued by infrared divergences [16, 17] that arise beyond a certain order in the coupling, rendering the expansion ill-defined. In the case of the pressure, this breakdown occurs at $O(g^6)$. Although the issue remains, through the thermal effective theories (see Section 3) the expansion can be reorganised in such a way that the infrared divergences are transparently isolated in the contributions at the ultrasoft scale. The hard and soft scales instead contribute through the matching coefficients, which are not sensitive to infrared physics.

The starting point for the perturbative determination of the pressure $p(T)$ is thus the decomposition in Eq. (21). The details of the calculation can be found in the literature (see e.g. Ref. [14] and references therein), and go beyond the scope of this Chapter. Nevertheless, from general arguments it is possible to infer characteristic features of perturbation theory at finite temperature, whose validity extends beyond the specific case of the calculation of the pressure.

- The term $c_E(T)$ represents the contribution from the hard modes. Its determination is part of the matching of EQCD to QCD. The only scale involved is $\sim \pi T$, and c_E , as well as the parameters in the EQCD Lagrangian, can be computed as a perturbative series in g^2 . By dimensional arguments, $c_E \sim (\pi T)^3$ thus we expect contributions at all even powers of g starting from $O(g^0)$.
- The term $c_M(T)$ represents the contribution from the soft modes. Its determination is part of the matching of MQCD to EQCD. The only scale involved is $m_E \sim gT$, and c_M , as well as the parameters in the MQCD Lagrangian, can be computed as a power series in terms of dimensionless ratios like g_E^2/m_E or λ_A/m_E . Notice in particular that odd powers of g arise in this expansion. By dimensional arguments, $c_M \sim m_E^3$ thus we expect contributions at all powers of g starting from $O(g^3)$.
- The last term in Eq. (21) represents the contribution from the ultrasoft modes, and as already mentioned it cannot be determined in perturbation theory. Nevertheless, since the only relevant scale is $g_M^2 \sim g^2 T$, we expect that contribution to be proportional to g_M^6 , with a non-perturbative coefficient. Therefore, it will enter the expansion starting from $O(g^6)$.

The pressure of hot QCD can be finally written as a power series in g [14],

$$\frac{p}{T^4} = \frac{8\pi^2}{45} \sum_k p_k \left(\frac{g}{2\pi}\right)^k, \quad (25)$$

where the coefficients p_k are known for $k = 0, 1, \dots, 5$, while the p_6 is partly known. The latter includes the non-perturbative effects of the ultrasoft scale [10] and a not yet determined perturbative contribution [18]. For reference, we report the coefficients up to one-loop order:

$$p_0 = 1 + \frac{21}{32} N_f, \quad p_1 = 0, \quad p_2 = -\frac{15}{4} \left(1 + \frac{5}{12} N_f\right). \quad (26)$$

The corrections to this result due to non-vanishing quark masses can be obtained from a perturbative calculation as well, and they have been determined to one-loop order [19].

Generally speaking, the validity of this perturbative expansion is tightly related to the regime of validity of the thermal effective theory, as discussed in Subsection 3.4. In practice, the convergence properties of the series are investigated by looking at the higher order corrections, which can be estimated for instance by comparing results at different perturbative orders or by varying the renormalization energy scale $\bar{\mu}$. A representation of the perturbative expansion of the entropy density (obtained from the pressure using Eq. (8)) for increasing orders is given in the left panel of Figure 2. The shadowed bands correspond to a variation of $\bar{\mu}$ by the factors 2 or 1/2 with respect to the central value

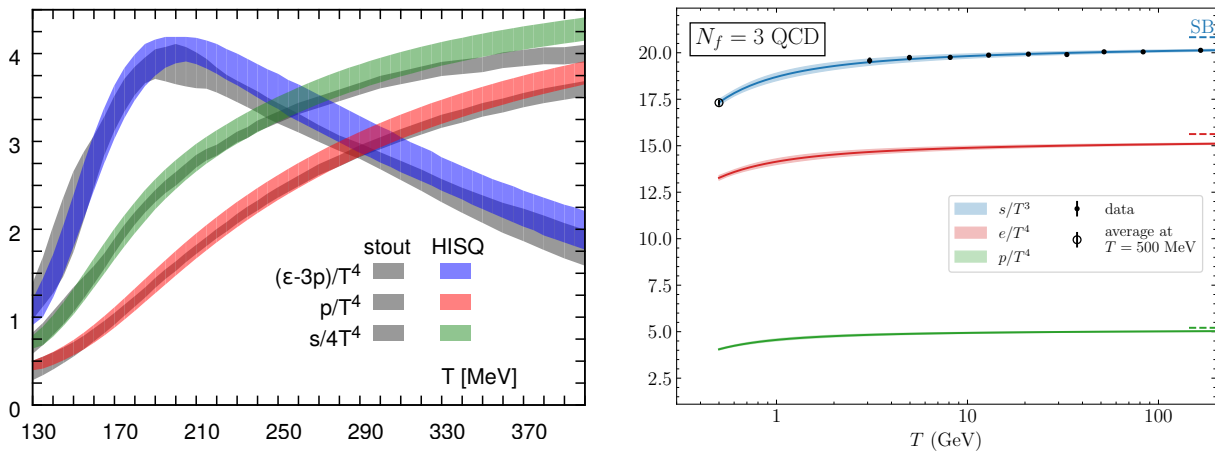


Fig. 1: Equation of State of QCD with three flavours. Left panel: results for the trace anomaly, pressure and entropy density in the interval 130 – 400 MeV determined in Refs. [22, 23]. Plot taken from Ref. [23]. Right panel: results for the entropy density, energy density and pressure for temperatures up to the electroweak scale [24, 25]. The value at 500 MeV is taken from Refs. [22, 26]. The dashed lines represent the Stefan-Boltzmann value of the three thermodynamic functions.

$\bar{\mu} = 2\pi T$. The poor agreement of the curves up to very high temperatures signals that higher order effects are relevant, and the convergence is slow at least up to temperatures of $O(100)$ GeV.

A mitigation of this behaviour has been obtained through a different approach to handle the infrared problem, called Hard Thermal Loop (HTL) perturbation theory [20, 21]. Building on the effective theory analysis, in the HTL framework two mass parameters are introduced, which represent the quark thermal mass and the Debye screening mass. The HTL perturbation expansion for the pressure has been computed to three-loop order, which is the last before the unavoidable infrared divergences manifest themselves. The right panel of Figure 2 represents the HTL prediction for the entropy density in the very high temperature regime, for increasing loop order. The shadowed bands give the dependence of the curves on the variation of $\bar{\mu}$ by the factors 2 and 1/2. At the electroweak scale, the agreement between the two highest orders is at the level of one combined sigma.

4.2 Non-perturbative determination

We discuss now the non-perturbative results for the EoS obtained using lattice QCD. The pressure is directly related to the partition function of the thermal system, and therefore it is defined up to an additive constant to be fixed with some prescription. The usual choice is that the pressure vanishes at vanishing temperature: $p(T = 0) = 0$. We can express the pressure as follows,

$$\frac{p(T)}{T^4} = \frac{p(T_0)}{T_0^4} + \int_{T_0}^T dT' \frac{I(T')}{(T')^5}, \quad (27)$$

where $I = e - 3p$ is the trace anomaly of the energy-momentum tensor, a quantity suitable for a lattice determination by computing expectation values of the pure gauge action and of the chiral condensate $\langle \bar{\psi}\psi \rangle$. The pressure can thus be obtained by integrating the trace anomaly, once the latter is known in the continuum limit for several values of the temperature. Given pressure and trace anomaly, the other functions follow from standard thermodynamic relations. The value $p(T_0)$ of the pressure at the (low) reference temperature T_0 can be estimated with low-energy models like the hadron resonance gas. This strategy is known as the integral method, and it was first used for the determination of the EoS in the SU(3) pure gauge theory [27]. In QCD, it has been applied to the determination of the EoS with $N_f = 2 + 1$ flavours (two light degenerate quarks and a heavier strange quark) [22, 23, 26], and with $N_f = 2 + 1 + 1$ flavours [28], up to temperatures of about 1 GeV.

Even if the integral method is well defined at all temperatures, for technical reasons a precise lattice calculation following this strategy becomes more and more costly from the computational point of view as the temperature increases. With the computing resources available to date, in practice the integral method is limited up to temperatures of the order of 1 GeV. More recently, a new strategy has been proposed [29, 30] that overcomes those limitations and allows to explore QCD non-perturbatively for temperatures up to the electroweak scale. According to this new method, the entropy density can be directly computed on the lattice by exploiting the Lorentz invariance of the theory [31–33]. The pressure is then determined by integrating the entropy in the temperature. Using this strategy the EoS has been determined for $N_f = 3$ QCD up to the electroweak scale [24, 25]. A summary of the determinations of the EoS with three flavours from different collaborations is represented in Figure 1.

The available non-perturbative results at very high temperatures allow us to confront with the perturbative expectations in a regime where the latter are supposed to work best. Figure 2 compares the results for the entropy density to perturbation theory in the standard approach (left panel) and in the HTL approach (right panel), as described in Subsection 4.1. If we consider both expansions up to the highest complete order ($O(g^5)$ for the left panel and NNLO for the right panel), then the agreement with the non-perturbative results is at the

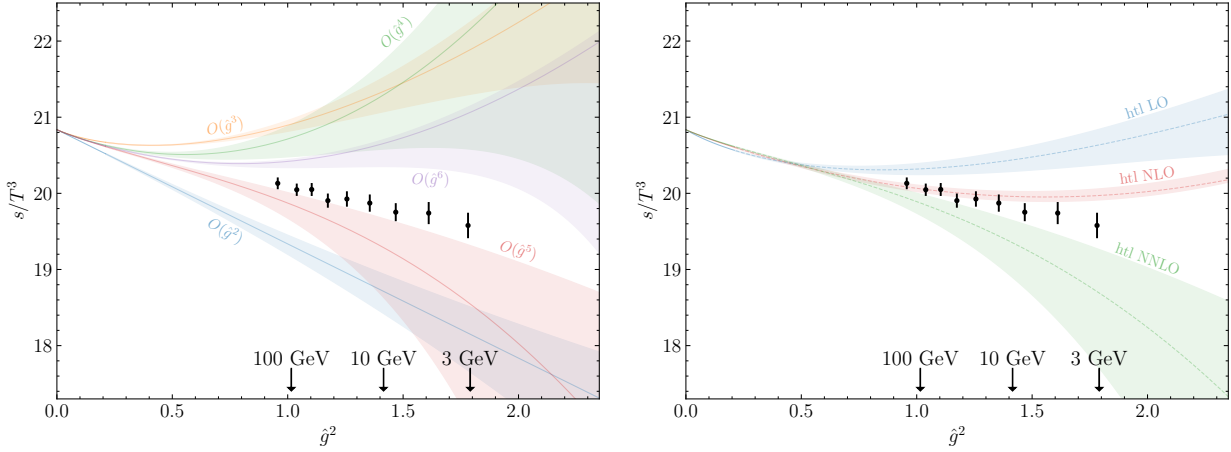


Fig. 2: Left panel: the non-perturbative results for the entropy density (black dots) from Refs. [24, 25] are compared to standard perturbation theory. Each curve includes up to the order in the strong coupling (here denoted by \hat{g}) reported by the label. Shaded bands correspond to a variation of the renormalization scale by the factors 2 or 1/2. Data are represented as a function of \hat{g} , and some values of the physical temperature are reported for reference. Right panel: the entropy density is compared to HTL perturbation theory at leading order (LO), next-to leading order (NLO) and next-to-next-to leading order (NNLO). Shaded bands have the same meaning as in the left panel.

level of one to two sigma, if the statistical error of the data is combined to the systematic one of the expansions due to the renormalization scale variation. However, a reliable estimation of the latter is difficult because of the oscillating behaviour of the expansions as the order increases.

4.3 Finite density

In perturbation theory, the non-zero density case can be treated in the limits of large temperature and small chemical potential, or vanishing temperature and large chemical potential [34–37]. Concerning non-perturbative methods, lattice QCD simulations cannot be carried out straightforwardly at a finite chemical potential, because the latter spoils the probabilistic interpretation of the Euclidean path integral on which the Monte Carlo sampling is based. This issue is known as the sign problem, and several strategies have been proposed to obtain results at finite density from the lattice at least under the approximation of small ratio μ/T : the reweighting method [38, 39], the Taylor expansion method [40], and the analytic continuation from imaginary chemical potential [41]. For the case of the EoS, the pressure can be Taylor expanded around $\mu/T = 0$,

$$\frac{p(T, \mu)}{T^4} = \sum_{n=0}^{\infty} \hat{p}_{2n}(T) \left(\frac{\mu}{T}\right)^{2n}, \quad \hat{p}_n(T) = \frac{1}{n!} \left. \frac{\partial^n (p/T^4)}{\partial (\mu/T)^n} \right|_{T, \mu=0}, \quad (28)$$

where the even powers only contribute because of the reflection symmetry of the partition function, $\mathcal{Z}(\mu) = \mathcal{Z}(-\mu)$. The coefficients \hat{p}_n are then expressed in terms of expectation values of local operators at vanishing chemical potential, that can be determined from lattice simulations [42–46].

5 Thermal phases of QCD

Strongly interacting matter behaves in qualitatively different ways as the temperature and density change. The various regimes as functions of T and μ are collected by the QCD phase diagram. Unfortunately, at present many properties of the latter remain at the conjectural level. On the theoretical side, lattice QCD has proven to be a powerful tool to explore the strong dynamics non-perturbatively at finite temperature and zero chemical potential. As discussed in Subsection 4.3, the sign problem limits the applicability of lattice QCD at non-vanishing density. Leveraging on asymptotic freedom, partial insights at very high temperatures or densities may come from perturbative approaches. On the experimental side, heavy-ion colliders probe the QCD plasma at temperatures up to a few hundreds MeV and up to the density of heavy nuclear matter. The study of compact astrophysical objects like neutron stars may help to chart the QCD phase diagram at values of baryon density that cannot be reached by particle physics experiments.

In the following Subsections we overview some established features of the QCD phase diagram, treating separately the cases of vanishing and non-vanishing chemical potential.

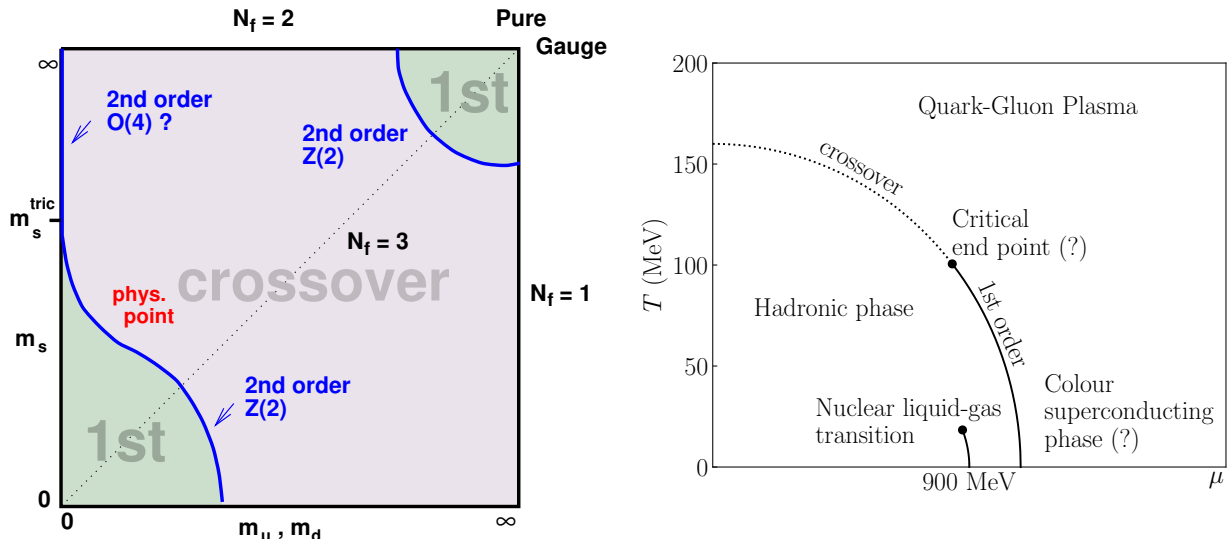


Fig. 3: Left: Columbia plot from Ref. [47]. Right: conjectured phase diagram of QCD.

5.1 The $\mu = 0$ case

There are experimental and theoretical evidences [48, 49] that, when the temperature increases, QCD matter undergoes a crossover from the ordinary hadronic matter to the so-called quark-gluon plasma, where the relevant degrees of freedom are strongly interacting quarks and gluons. For this reason the two regimes are also known as confined and deconfined phase, respectively. The pseudocritical temperature at which the crossover occurs is $T_{pc} \sim 160$ MeV, and it has been estimated in lattice QCD [50, 51].

The nature of this change of regime is better understood if we consider its dependence on the quark masses, with the help of the Columbia plot [47, 52] in the left panel of Figure 3. On the horizontal axis it appears the mass of the light (up and down) quarks, taken to be degenerate, while the vertical axis is for the strange quark mass. At energies of the order of T_{pc} , the charm, bottom and top quarks can be considered as static colour sources and excluded from this analysis.

Let's start from the top-right corner of Figure 3, i.e. QCD with infinitely heavy quarks. In this scenario all the quarks decouple and QCD behaves as the SU(3) pure gauge theory. The latter is known to have a first order phase transition due to the spontaneous breaking of the Z_3 symmetry, which is the center of the gauge group [53]. The related critical temperature $T_c \sim 300$ MeV has been determined by non-perturbative calculations on the lattice [54–56]. Although the pure gauge theory is unphysical, the value of T_c provides a useful order of magnitude estimate.

Dynamical quarks break explicitly the Z_3 symmetry. If we allow for a smooth dependence of the latent heat on the quark masses, the pure gauge point will be surrounded by a region of first order transition (light green at the top-right corner). As we lower the quark masses, the phase transition becomes weaker and weaker till it vanishes along a critical line of second order phase transition (the blue line). The light grey region of the plot is characterised by the absence of a phase transition. The low and high temperature phases are smoothly connected by a crossover at some pseudo-critical temperature T_{pc} , which is in general a function of the quark masses. As we mentioned before, the physical point falls within this regime.

For vanishing quark masses (bottom-left corner) the relevant symmetry is chiral symmetry. In QCD at the chiral point ($m_u = m_d = m_s = 0$) the non-singlet axial generators of chiral symmetry are spontaneously broken at zero temperature. It has been shown from lattice calculations that this symmetry is restored as the temperature increases [57, 58]. It is however not clear how the restoration occurs: the prediction of a first order phase transition for $N_f \geq 3$ [59] has not been confirmed yet (nor completely ruled out) by non-perturbative calculations [60].

Finally, the situation is not yet settled also on the left edge of the Columbia plot, where $m_u = m_d = 0$ and $m_s > 0$. In that case the nature of the transition depends on the anomalous U(1) axial symmetry and on the non-singlet axial generators of the two-flavour chiral group [61, 62]. For sufficiently high strange quark mass, the restoration of the non-singlet axial generators should lead to a second order phase transition (as reported in Figure 3). If however the axial anomaly is suppressed at the critical temperature, then the transition could be either first or second order. Non-perturbative explorations of this issue are ongoing, see Refs. [60, 63–65] for recent results.

5.2 The $\mu \neq 0$ case

The non-zero chemical potential introduces in principle one extra axis to the picture described for $\mu = 0$. If we set the light and strange quark masses to their physical values, the resulting conjectured phase diagram of QCD is represented, in the $T - \mu$ plane, in the right panel of Figure 3. A huge effort is devoted to the characterisation of the (pseudo)critical line that separates the hadronic and plasma phases. The

curvature can be expressed as a change in the temperature T_{pc} at non-vanishing chemical potential. For small μ/T we can expand as follows,

$$\frac{T_{pc}(\mu)}{T_{pc}(0)} = 1 - \kappa_2 \left(\frac{\mu}{T_{pc}(0)} \right)^2 - \kappa_4 \left(\frac{\mu}{T_{pc}(0)} \right)^4 + \dots, \quad (29)$$

and the coefficients κ_2, κ_4 have been determined from lattice QCD calculations by studying the μ -dependence of observables that are sensitive to the change of regime [50, 51, 66, 67]. It is believed that the crossover becomes stronger and stronger for increasing chemical potential, and that for sufficiently high μ it will eventually turn into a first order phase transition. The two regimes should be linked by a critical point in the phase diagram. No clear signs of the existence of the critical point have been observed yet, both from theory and experiments (recent updates in Refs. [68, 69]). At lower temperatures, the nuclear liquid-gas coexistence line at $\mu \sim 920$ MeV ends with a critical point at a temperature of about 18 MeV [70]. In the high density region, the appearance of new exotic states of QCD matter is expected [71]. Even if some indirect insights may be obtained from the study of neutron stars [72], our knowledge of the phase diagram in that regime is limited by the fact that strong interactions at very high density cannot be explored by experiments in terrestrial laboratories.

6 Summary

This Chapter introduces the foundations of QCD thermodynamics. The starting point is the grand-canonical partition function for strongly interacting particles, and its representation in the Euclidean path integral formalism. The temperature T enters as a compact time direction of length $1/T$, and the ordinary vacuum QCD is recovered in the limit $T \rightarrow 0$. The pressure is directly related to the partition function, while taking derivatives with respect to T and the chemical potential μ yields other fundamental thermodynamic functions collectively known as the Equation of State.

At high temperature, thermal screening effects emerge [8, 9]. QCD degrees of freedom separate into hard, soft and ultrasoft modes, respectively screened at the distances $\sim (\pi T)^{-1}$, $\sim (gT)^{-1}$ and $\sim (g^2 T)^{-1}$. Harder modes can be integrated out using effective field theories, leaving simpler descriptions at large distances. This scale separation leads to an effective decomposition of the QCD partition function into contributions from each thermal scale.

These screening effects are responsible of the infrared divergences that spoil the weak coupling expansions in thermal QCD [16]. Partial improvement is obtained by resumming the expansion using effective theory methods [14], though the perturbative series still converges poorly even at electroweak temperatures. This motivates alternative approaches such as the hard thermal loop perturbation theory [20, 21].

Non-perturbative lattice QCD remains crucial for the investigation of QCD at all temperatures. As an example, we have summarised the results obtained for the Equation of State [22, 23, 25, 26, 28], but in principle several other properties of the QCD plasma can be explored, like hadronic screening lengths or transport coefficients [73]. Extending lattice QCD to non-zero chemical potential is non-trivial because of the sign problem, though results for small μ/T can be obtained.

Despite major progress in understanding QCD thermodynamics, several open questions remain about its phase diagram. At low density, increasing temperature induces a smooth crossover from the hadronic matter to the quark-gluon plasma. At high density, this may become a first order transition, potentially with a critical point, though no definitive evidence exists. The very high density regions, which are inaccessible to colliders or lattice methods, remain largely unexplored. The hope is that the remarkable advances achieved in recent years in the observation and characterisation of compact astrophysical objects [72], may provide some information on the properties of cold and dense QCD matter.

Acknowledgement

I wish to thank Michele Pepe for valuable comments on the manuscript of this Chapter.

References

- [1] S. Acharya, et al., Two-particle transverse momentum correlations in pp and p-Pb collisions at LHC energies, *Phys. Rev. C* 107 (5) (2023) 054617. [arXiv:2211.08979](https://arxiv.org/abs/2211.08979), [doi:10.1103/PhysRevC.107.054617](https://doi.org/10.1103/PhysRevC.107.054617).
- [2] M. Gyulassy, L. McLerran, New forms of QCD matter discovered at RHIC, *Nucl. Phys. A* 750 (2005) 30–63. [arXiv:nuc1-th/0405013](https://arxiv.org/abs/nuc1-th/0405013), [doi:10.1016/j.nuclphysa.2004.10.034](https://doi.org/10.1016/j.nuclphysa.2004.10.034).
- [3] K. Saikawa, S. Shirai, Primordial gravitational waves, precisely: The role of thermodynamics in the Standard Model, *JCAP* 05 (2018) 035. [arXiv:1803.01038](https://arxiv.org/abs/1803.01038), [doi:10.1088/1475-7516/2018/05/035](https://doi.org/10.1088/1475-7516/2018/05/035).
- [4] K. Saikawa, S. Shirai, Precise WIMP Dark Matter Abundance and Standard Model Thermodynamics, *JCAP* 08 (2020) 011. [arXiv:2005.03544](https://arxiv.org/abs/2005.03544), [doi:10.1088/1475-7516/2020/08/011](https://doi.org/10.1088/1475-7516/2020/08/011).
- [5] I. Montvay, G. Munster, *Quantum fields on a lattice*, Cambridge Monographs on Mathematical Physics, Cambridge University Press, 1997. [doi:10.1017/CB09780511470783](https://doi.org/10.1017/CB09780511470783).
- [6] H. J. Rothe, *Lattice Gauge Theories : An Introduction (Fourth Edition)*, Vol. 43, World Scientific Publishing Company, 2012. [doi:10.1142/8229](https://doi.org/10.1142/8229).
- [7] J. I. Kapusta, C. Gale, *Finite-Temperature Field Theory : Principles and Applications*, 2nd edition, Cambridge University Press, 2007. [doi:10.1017/9781009401968](https://doi.org/10.1017/9781009401968).

- [8] T. Appelquist, R. D. Pisarski, High-Temperature Yang-Mills Theories and Three-Dimensional Quantum Chromodynamics, *Phys. Rev. D* 23 (1981) 2305. doi:10.1103/PhysRevD.23.2305.
- [9] E. Braaten, A. Nieto, Free energy of QCD at high temperature, *Phys. Rev. D* 53 (1996) 3421–3437. arXiv:hep-ph/9510408, doi:10.1103/PhysRevD.53.3421.
- [10] A. Hietanen, K. Kajantie, M. Laine, K. Rummukainen, Y. Schroder, Plaquette expectation value and gluon condensate in three dimensions, *JHEP* 01 (2005) 013. arXiv:hep-lat/0412008, doi:10.1088/1126-6708/2005/01/013.
- [11] A. Hietanen, K. Kajantie, M. Laine, K. Rummukainen, Y. Schroder, Three-dimensional physics and the pressure of hot QCD, *Phys. Rev. D* 79 (2009) 045018. arXiv:0811.4664, doi:10.1103/PhysRevD.79.045018.
- [12] S. Nadkarni, Dimensional Reduction in Finite Temperature Quantum Chromodynamics. 2., *Phys. Rev. D* 38 (1988) 3287. doi:10.1103/PhysRevD.38.3287.
- [13] N. P. Landsman, Limitations to Dimensional Reduction at High Temperature, *Nucl. Phys. B* 322 (1989) 498–530. doi:10.1016/0550-3213(89)90424-0.
- [14] K. Kajantie, M. Laine, K. Rummukainen, Y. Schroder, The Pressure of hot QCD up to $g_6 \ln(1/g)$, *Phys. Rev. D* 67 (2003) 105008. arXiv:hep-ph/0211321, doi:10.1103/PhysRevD.67.105008.
- [15] M. Bruno, M. Dalla Brida, P. Fritzsche, T. Korzec, A. Ramos, S. Schaefer, H. Simma, S. Sint, R. Sommer, QCD Coupling from a Nonperturbative Determination of the Three-Flavor Λ Parameter, *Phys. Rev. Lett.* 119 (10) (2017) 102001. arXiv:1706.03821, doi:10.1103/PhysRevLett.119.102001.
- [16] A. D. Linde, Infrared Problem in Thermodynamics of the Yang-Mills Gas, *Phys. Lett. B* 96 (1980) 289–292. doi:10.1016/0370-2693(80)90769-8.
- [17] D. J. Gross, R. D. Pisarski, L. G. Yaffe, QCD and Instantons at Finite Temperature, *Rev. Mod. Phys.* 53 (1981) 43. doi:10.1103/RevModPhys.53.43.
- [18] P. Navarrete, Y. Schröder, The g^6 pressure of hot Yang-Mills theory: canonical form of the integrand, *JHEP* 11 (2024) 037. arXiv:2408.15830, doi:10.1007/JHEP11(2024)037.
- [19] M. Laine, Y. Schroder, Quark mass thresholds in QCD thermodynamics, *Phys. Rev. D* 73 (2006) 085009. arXiv:hep-ph/0603048, doi:10.1103/PhysRevD.73.085009.
- [20] J. O. Andersen, M. Strickland, N. Su, Three-loop HTL gluon thermodynamics at intermediate coupling, *JHEP* 08 (2010) 113. arXiv:1005.1603, doi:10.1007/JHEP08(2010)113.
- [21] J. O. Andersen, L. E. Leganger, M. Strickland, N. Su, Three-loop HTL QCD thermodynamics, *JHEP* 08 (2011) 053. arXiv:1103.2528, doi:10.1007/JHEP08(2011)053.
- [22] S. Borsanyi, Z. Fodor, C. Hoelbling, S. D. Katz, S. Krieg, K. K. Szabo, Full result for the QCD equation of state with 2+1 flavors, *Phys. Lett. B* 730 (2014) 99–104. arXiv:1309.5258, doi:10.1016/j.physletb.2014.01.007.
- [23] A. Bazavov, et al., Equation of state in (2+1)-flavor QCD, *Phys. Rev. D* 90 (2014) 094503. arXiv:1407.6387, doi:10.1103/PhysRevD.90.094503.
- [24] M. Bresciani, M. D. Brida, L. Giusti, M. Pepe, QCD Equation of State with $N_f=3$ Flavors up to the Electroweak Scale, *Phys. Rev. Lett.* 134 (20) (2025) 201904. arXiv:2501.11603, doi:10.1103/PhysRevLett.134.201904.
- [25] M. Bresciani, M. D. Brida, L. Giusti, M. Pepe, QCD Equation of State at very high temperature: computational strategy, simulations and data analysis (11 2025). arXiv:2511.09160.
- [26] A. Bazavov, P. Petreczky, J. H. Weber, Equation of State in 2+1 Flavor QCD at High Temperatures, *Phys. Rev. D* 97 (1) (2018) 014510. arXiv:1710.05024, doi:10.1103/PhysRevD.97.014510.
- [27] G. Boyd, J. Engels, F. Karsch, E. Laermann, C. Legeland, M. Lutgemeier, B. Petersson, Thermodynamics of SU(3) lattice gauge theory, *Nucl. Phys. B* 469 (1996) 419–444. arXiv:hep-lat/9602007, doi:10.1016/0550-3213(96)00170-8.
- [28] S. Borsanyi, et al., Calculation of the axion mass based on high-temperature lattice quantum chromodynamics, *Nature* 539 (7627) (2016) 69–71. arXiv:1606.07494, doi:10.1038/nature20115.
- [29] L. Giusti, M. Pepe, Equation of state of the SU(3) Yang–Mills theory: A precise determination from a moving frame, *Phys. Lett. B* 769 (2017) 385–390. arXiv:1612.00265, doi:10.1016/j.physletb.2017.04.001.
- [30] M. Dalla Brida, L. Giusti, T. Harris, D. Laudicina, M. Pepe, Non-perturbative thermal QCD at all temperatures: the case of mesonic screening masses, *JHEP* 04 (2022) 034. arXiv:2112.05427, doi:10.1007/JHEP04(2022)034.
- [31] L. Giusti, H. B. Meyer, Thermal momentum distribution from path integrals with shifted boundary conditions, *Phys. Rev. Lett.* 106 (2011) 131601. arXiv:1011.2727, doi:10.1103/PhysRevLett.106.131601.
- [32] L. Giusti, H. B. Meyer, Thermodynamic potentials from shifted boundary conditions: the scalar-field theory case, *JHEP* 11 (2011) 087. arXiv:1110.3136, doi:10.1007/JHEP11(2011)087.
- [33] L. Giusti, H. B. Meyer, Implications of Poincare symmetry for thermal field theories in finite-volume, *JHEP* 01 (2013) 140. arXiv:1211.6669, doi:10.1007/JHEP01(2013)140.
- [34] B. A. Freedman, L. D. McLerran, Fermions and Gauge Vector Mesons at Finite Temperature and Density. 3. The Ground State Energy of a Relativistic Quark Gas, *Phys. Rev. D* 16 (1977) 1169. doi:10.1103/PhysRevD.16.1169.
- [35] A. Vuorinen, The Pressure of QCD at finite temperatures and chemical potentials, *Phys. Rev. D* 68 (2003) 054017. arXiv:hep-ph/0305183, doi:10.1103/PhysRevD.68.054017.
- [36] A. Ipp, K. Kajantie, A. Rebhan, A. Vuorinen, The Pressure of deconfined QCD for all temperatures and quark chemical potentials, *Phys. Rev. D* 74 (2006) 045016. arXiv:hep-ph/0604060, doi:10.1103/PhysRevD.74.045016.
- [37] N. Haque, J. O. Andersen, M. G. Mustafa, M. Strickland, N. Su, Three-loop pressure and susceptibility at finite temperature and density from hard-thermal-loop perturbation theory, *Phys. Rev. D* 89 (6) (2014) 061701. arXiv:1309.3968, doi:10.1103/PhysRevD.89.061701.
- [38] A. M. Ferrenberg, R. H. Swendsen, New Monte Carlo Technique for Studying Phase Transitions, *Phys. Rev. Lett.* 61 (1988) 2635–2638. doi:10.1103/PhysRevLett.61.2635.
- [39] Z. Fodor, S. D. Katz, A New method to study lattice QCD at finite temperature and chemical potential, *Phys. Lett. B* 534 (2002) 87–92. arXiv:hep-lat/0104001, doi:10.1016/S0370-2693(02)01583-6.
- [40] C. R. Allton, S. Ejiri, S. J. Hands, O. Kaczmarek, F. Karsch, E. Laermann, C. Schmidt, L. Scorzato, The QCD thermal phase transition in the presence of a small chemical potential, *Phys. Rev. D* 66 (2002) 074507. arXiv:hep-lat/0204010, doi:10.1103/PhysRevD.66.074507.
- [41] M. D’Elia, M.-P. Lombardo, Finite density QCD via imaginary chemical potential, *Phys. Rev. D* 67 (2003) 014505. arXiv:hep-lat/0209146, doi:10.1103/PhysRevD.67.014505.
- [42] S. Borsanyi, G. Endrodi, Z. Fodor, S. D. Katz, S. Krieg, C. Ratti, K. K. Szabo, QCD equation of state at nonzero chemical potential: continuum results with physical quark masses at order mu^2 , *JHEP* 08 (2012) 053. arXiv:1204.6710, doi:10.1007/JHEP08(2012)053.
- [43] R. Bellwied, S. Borsanyi, Z. Fodor, S. D. Katz, A. Pasztor, C. Ratti, K. K. Szabo, Fluctuations and correlations in high temperature QCD, *Phys. Rev. D* 92 (11) (2015) 114505. arXiv:1507.04627, doi:10.1103/PhysRevD.92.114505.

- [44] M. D'Elia, G. Gagliardi, F. Sanfilippo, Higher order quark number fluctuations via imaginary chemical potentials in $N_f = 2 + 1$ QCD, *Phys. Rev. D* 95 (9) (2017) 094503. arXiv:1611.08285, doi:10.1103/PhysRevD.95.094503.
- [45] A. Bazavov, et al., Skewness, kurtosis, and the fifth and sixth order cumulants of net baryon-number distributions from lattice QCD confront high-statistics STAR data, *Phys. Rev. D* 101 (7) (2020) 074502. arXiv:2001.08530, doi:10.1103/PhysRevD.101.074502.
- [46] S. Borsanyi, Z. Fodor, J. N. Guenther, S. D. Katz, P. Parotto, A. Pasztor, D. Pesznyak, K. K. Szabo, C. H. Wong, Continuum-extrapolated high-order baryon fluctuations, *Phys. Rev. D* 110 (1) (2024) L011501. arXiv:2312.07528, doi:10.1103/PhysRevD.110.L011501.
- [47] O. Philipsen, Lattice QCD at non-zero temperature and baryon density, in: *Les Houches Summer School: Session 93: Modern perspectives in lattice QCD: Quantum field theory and high performance computing*, 2010, pp. 273–330. arXiv:1009.4089.
- [48] J. W. Harris, B. Müller, "QGP Signatures" Revisited, *Eur. Phys. J. C* 84 (3) (2024) 247. arXiv:2308.05743, doi:10.1140/epjc/s10052-024-12533-y.
- [49] Y. Aoki, G. Endrodi, Z. Fodor, S. D. Katz, K. K. Szabo, The Order of the quantum chromodynamics transition predicted by the standard model of particle physics, *Nature* 443 (2006) 675–678. arXiv:hep-lat/0611014, doi:10.1038/nature05120.
- [50] A. Bazavov, et al., Chiral crossover in QCD at zero and non-zero chemical potentials, *Phys. Lett. B* 795 (2019) 15–21. arXiv:1812.08235, doi:10.1016/j.physletb.2019.05.013.
- [51] S. Borsanyi, Z. Fodor, J. N. Guenther, R. Kara, S. D. Katz, P. Parotto, A. Pasztor, C. Ratti, K. K. Szabo, QCD Crossover at Finite Chemical Potential from Lattice Simulations, *Phys. Rev. Lett.* 125 (5) (2020) 052001. arXiv:2002.02821, doi:10.1103/PhysRevLett.125.052001.
- [52] F. R. Brown, F. P. Butler, H. Chen, N. H. Christ, Z.-h. Dong, W. Schaffer, L. I. Unger, A. Vaccarino, On the existence of a phase transition for QCD with three light quarks, *Phys. Rev. Lett.* 65 (1990) 2491–2494. doi:10.1103/PhysRevLett.65.2491.
- [53] L. G. Yaffe, B. Svetitsky, First Order Phase Transition in the SU(3) Gauge Theory at Finite Temperature, *Phys. Rev. D* 26 (1982) 963. doi:10.1103/PhysRevD.26.963.
- [54] T. Celik, J. Engels, H. Satz, The Latent Heat of Deconfinement in SU(3) Yang-Mills Theory, *Phys. Lett. B* 129 (1983) 323–327. doi:10.1016/0370-2693(83)90675-5.
- [55] S. Borsanyi, K. R., Z. Fodor, D. A. Godzieba, P. Parotto, D. Sexty, Precision study of the continuum SU(3) Yang-Mills theory: How to use parallel tempering to improve on supercritical slowing down for first order phase transitions, *Phys. Rev. D* 105 (7) (2022) 074513. arXiv:2202.05234, doi:10.1103/PhysRevD.105.074513.
- [56] L. Giusti, M. Hirasawa, M. Pepe, L. Virzi, A precise study of the thermodynamic properties of the SU(3) Yang-Mills theory across the deconfinement transition, *Phys. Lett. B* 868 (2025) 139775. arXiv:2501.10284, doi:10.1016/j.physletb.2025.139775.
- [57] A. Bazavov, et al., The chiral transition and $U(1)_A$ symmetry restoration from lattice QCD using Domain Wall Fermions, *Phys. Rev. D* 86 (2012) 094503. arXiv:1205.3535, doi:10.1103/PhysRevD.86.094503.
- [58] D. Laudicina, M. Dalla Brida, L. Giusti, T. Harris, M. Pepe, QCD mesonic screening masses and restoration of chiral symmetry at high T, *PoS LATTICE2022* (2023) 182. arXiv:2212.02167, doi:10.22323/1.430.0182.
- [59] R. D. Pisarski, F. Wilczek, Remarks on the Chiral Phase Transition in Chromodynamics, *Phys. Rev. D* 29 (1984) 338–341. doi:10.1103/PhysRevD.29.338.
- [60] F. Cuteri, O. Philipsen, A. Sciarra, On the order of the QCD chiral phase transition for different numbers of quark flavours, *JHEP* 11 (2021) 141. arXiv:2107.12739, doi:10.1007/JHEP11(2021)141.
- [61] A. Butti, A. Pelissetto, E. Vicari, On the nature of the finite temperature transition in QCD, *JHEP* 08 (2003) 029. arXiv:hep-ph/0307036, doi:10.1088/1126-6708/2003/08/029.
- [62] A. Pelissetto, E. Vicari, Relevance of the axial anomaly at the finite-temperature chiral transition in QCD, *Phys. Rev. D* 88 (10) (2013) 105018. arXiv:1309.5446, doi:10.1103/PhysRevD.88.105018.
- [63] B. B. Brandt, A. Francis, H. B. Meyer, O. Philipsen, D. Robaina, H. Wittig, On the strength of the $U_A(1)$ anomaly at the chiral phase transition in $N_f = 2$ QCD, *JHEP* 12 (2016) 158. arXiv:1608.06882, doi:10.1007/JHEP12(2016)158.
- [64] H. T. Ding, et al., Chiral Phase Transition Temperature in $(2+1)$ -Flavor QCD, *Phys. Rev. Lett.* 123 (6) (2019) 062002. arXiv:1903.04801, doi:10.1103/PhysRevLett.123.062002.
- [65] A. Y. Kotov, M. P. Lombardo, A. Trunin, QCD transition at the physical point, and its scaling window from twisted mass Wilson fermions, *Phys. Lett. B* 823 (2021) 136749. arXiv:2105.09842, doi:10.1016/j.physletb.2021.136749.
- [66] C. Bonati, M. D'Elia, F. Negro, F. Sanfilippo, K. Zambello, Curvature of the pseudocritical line in QCD: Taylor expansion matches analytic continuation, *Phys. Rev. D* 98 (5) (2018) 054510. arXiv:1805.02960, doi:10.1103/PhysRevD.98.054510.
- [67] A. Smecca, G. Aarts, C. Allton, R. Bignell, B. Jäger, S.-i. Nam, S. Kim, J.-I. Skullerud, L.-K. Wu, Curvature of the pseudocritical line in the QCD phase diagram from mesonic lattice correlation functions, *Phys. Rev. D* 112 (11) (2025) 114509. arXiv:2412.20922, doi:10.1103/wjm8-4smh.
- [68] S. Borsanyi, Z. Fodor, J. N. Guenther, P. Parotto, A. Pasztor, C. Ratti, V. Vovchenko, C. H. Wong, Lattice QCD constraints on the critical point from an improved precision equation of state, *Phys. Rev. D* 112 (11) (2025) L111505. arXiv:2502.10267, doi:10.1103/rj6r-dmg9.
- [69] B. E. Aboona, et al., Precision Measurement of Net-Proton-Number Fluctuations in Au+Au Collisions at RHIC, *Phys. Rev. Lett.* 135 (14) (2025) 142301. arXiv:2504.00817, doi:10.1103/9169-2d7p.
- [70] J. B. Elliott, P. T. Lake, L. G. Moretto, L. Phair, Determination of the coexistence curve, critical temperature, density, and pressure of bulk nuclear matter from fragment emission data, *Phys. Rev. C* 87 (5) (2013) 054622. doi:10.1103/PhysRevC.87.054622.
- [71] T. Schäfer, E. V. Shuryak, Phases of QCD at high baryon density, *Lect. Notes Phys.* 578 (2001) 203–217. arXiv:nuc1-th/0010049.
- [72] R. Kumar, et al., Theoretical and experimental constraints for the equation of state of dense and hot matter, *Living Rev. Rel.* 27 (1) (2024) 3. arXiv:2303.17021, doi:10.1007/s41114-024-00049-6.
- [73] H. B. Meyer, Transport Properties of the Quark-Gluon Plasma: A Lattice QCD Perspective, *Eur. Phys. J. A* 47 (2011) 86. arXiv:1104.3708, doi:10.1140/epja/i2011-11086-3.